International Journal of Modern Manufacturing Technologies
ISSN 2067–3604, Vol. XVII, No. 3 / 2025
https://doi.org/ 10.54684/ijmmt.2025.17.3.29

NUMERICAL SIMULATION OF INDENTATION OF A MAXWELL VISCOELASTIC HALF-SPACE

Delia Cerlinca[1,2], Sergiu Spinu[1,2]

[1] Department of Mechanics and Technologies, Stefan cel Mare University of Suceava,
13th University Street, 720229, Romania
[2] Integrated Center for Research, Development and Innovation in Advanced Materials, Nanotechnologies, and Distributed Systems for Fabrication and Control (MANSiD), Stefan cel Mare University, Suceava, Romania

Corresponding author: Sergiu Spinu, sergiu.spinu@fim.usv.ro

Abstract: Automotive belts, tires and various biomedical devices have components made of elastomers and rubbers, and their mechanical behaviour description is best performed in the frame of viscoelasticity. Assessing the performance of mechanical contacts between viscoelastic materials lacks general analytical solutions, inviting numerical analysis to predict the contact response of materials with mathematically complex mechanical properties. Semi-analytical methods are reliable and efficient tools for contact modelling, either elastic or elastic-plastic. Viscoelastic contact processes can also be considered, provided linear viscoelasticity is assumed, and a temporal discretization is imposed to capture the time-variable properties of the viscoelastic material. Using a similar approach to that for purely elastic contacts, pressure-induced displacement can be expressed by the superposition of effects of discrete pressures from the current step, but also from the precedent time step, leading to a recurrent displacement formulation. The contact problem needs to be solved at any time point from the load path, replicating the contact process and the memory effect of the viscoelastic material. The temporal discretization should be chosen with respect to the gradients in the viscoelastic properties, but also to those from the loading history, so that both the viscoelastic properties and the pressure distribution can be assumed constant in each time interval. The Maxwell unit is largely used in the modelling of viscoelastic materials, and the study of indentation of a Maxwell half-space by a rigid sphere may advance the understanding of viscoelastic contact processes. Even when the same Maxwell parameters are imposed, the contact evolution depends strongly on the loading path, due to the memory effect. Various loading histories are imposed in this paper, including step, ramped, sine or pulsatile loading, and the contact parameters are obtained through numerical simulation. The evolutions of maximum pressure and contact radius with the load are depicted in each case. For non-monotonic and cyclic loadings, it is predicted that a delay exists between the extremums of load and those of the rigid-body approach and contact radius. This out-of-phase response leads to a steady increase in the maximum contact parameters in cyclic loading, although a stationary regime may be established for different ratios between the load frequency and the relaxation time of the Maxwell material. The conducted simulations prove that the applied simulation technique is robust enough to capture the specifics of all potential contact cases involving viscoelastic materials.

Key words: viscoelastic contact, semi-analytical method, Maxwell model, indentation.

1. INTRODUCTION

Electrical insulations, seals, belts, or tires are used in various engineering fields, such as automotive, and the mechanical behaviour description of their materials must take into account the time-dependent properties specific to viscoelasticity. Developing explicit relations for the contact processes involving these types of materials is problematic if not impossible, and initial solutions [1] were derived by analogy with the elastic contact case. The approach was based on the fact that, when the Laplace transform was applied to the equations of the viscoelastic contact problem, the time parameter was removed in the transformed domain, and the transformed equations had a similar structure to their elastic counterparts. This invites the construction of viscoelastic solutions by analogy, but additional difficulties arise in the treatment of varying boundary conditions, which lead to solutions of limited applicability, such as monotonically increasing contact area. These authors [2-4] contributed to the removal of some of the initial limitations, but a general viscoelastic contact solution was not attained.

On the other hand, semi-analytical methods emerged as robust and efficient tools to solve elastic contact problems [5,6]. Adding a load path discretization resulted [7,8] in a solution for the elastic-plastic contact problem, although the time parameter was not explicitly taken into account. For viscoelasticity, a temporal discretization can replicate [9] the memory effect of the viscoelastic material. The latter discretization should be fine enough so that, from

one time increment to the next, not only the viscoelastic properties, but also the load, do not vary by a great amount. The viscoelastic indentation was also studied by these authors [10-12].
This paper continues a previous work by the same authors [13], by studying the indentation of a viscoelastic Maxwell half-space with various loading paths. The evolution of the contact parameters is replicated by numerical simulation. For monotonically increasing contact radii, the results are verified against literature [14]. The specifics of each type of loading history are discussed, and the out-of-phase response between load and rigid-body approach is shown for a pulsatile load. The presented simulations attest to the computer code as a robust instrument for contact modelling and simulation.

2. MATERIALS AND METHODS

Unlike elastic materials, whose mechanical response is time and loading path-independent, the viscoelastic ones exhibit time-dependent responses, adding a new parameter in the problem's mathematical model. The functions of time introduced to characterize this continuously changing behaviour are the relaxation modulus $\psi(t)$, i.e. the ratio of a time-dependent stress $\sigma(t)$ over a constant strain ε_0, and the creep compliance function $\varphi(t)$, i.e., as the ratio of a time-dependent strain $\varepsilon(t)$ and a constant stress σ_0:

$$\psi(t) = \frac{\sigma(t)}{\varepsilon_0}; \quad \varphi(t) = \frac{\varepsilon(t)}{\sigma_0}. \tag{1}$$

These functions express a feature observed in many experiments: in a uniaxial test, less stress is needed to preserve the same amount of strain, thus material relaxation sets in, whereas when subjected to constant stress, the strain increases with time. Considering these features of the viscoelastic material, the simplest manner to model a viscoelastic material is by a spring and a dashpot connected in series, i.e., a Maxwell model. The latter is described by the following functions:

$$\psi(t) = \frac{1}{g} + \frac{t}{\eta}; \quad \varphi(t) = g \cdot \exp(-t/\tau), \tag{2}$$

with g the spring stiffness, η the dashpot viscosity, and $\tau = \eta/g$ the relaxation time. To further model a broader spectrum of relaxation times, one can connect in parallel a number n Maxwell models with various stiffnesses and viscosities, and a single spring g_0, yielding a so-called generalised Maxwell model, whose relaxation modulus can be expressed as:

$$\psi(t) = \left[g_0 + \sum_{i=1}^{n} g_i \exp\left(-\frac{t\eta_i}{g_i} \right) \right] H(t), \tag{3}$$

with $H(t)$ the Heaviside step function. The response to arbitrary histories of strain or of stress can be further derived by integration, implying decomposition of loading history into infinitesimal steps and linear viscoelasticity allowing superposition:

$$\sigma(t) = \int_0^t \psi(t-t') \frac{\partial \varepsilon(t')}{\partial t'} dt', \tag{4}$$

$$\varepsilon(t) = \int_0^t \varphi(t-t') \frac{\partial \sigma(t')}{\partial t'} dt'. \tag{5}$$

Based on these assumptions, the solution of a viscoelastic contact problem was approached in the following manner by Radok and Lee [1]: they observed that, by transforming a viscoelastic contact model into the Laplace or Fourier domains, the time parameter is removed and equations having the same structure as their purely elastic counterparts are obtained. Thus, they forced elastic solutions into the viscoelastic model in the frame of a so-called elastic-viscoelastic correspondence principle, stating that viscoelastic solutions can be attained by swapping the elastic modulus from the equivalent elastic problem with the creep compliance function. The application of the latter technique is limited by the continuously varying boundaries conditions in the contact problem, and is restricted to continuously growing contact area. Radok and Lee [1] pointed out the method limitations, stating that false negative pressure is predicted in case of load decrease. Some of the model limitations were subsequently removed by Ting [3,4].

In this framework, Ciornei [14] expressed the time-dependent contact area and pressure distribution in the spherical, axisymmetric indentation of a Maxwell viscoelastic half-space by a rigid sphere, with various loading histories. For example, a rigid sphere of radius R pressed against a viscoelastic Maxwell half-space in step loading $W(t)=W_{\max}H(t)$ yields a contact radius $a(t)$ and a rigid body-approach $\omega(t)$:

$$a(t)=\left[\frac{3RW_{\max}}{16g}\left(1+\frac{t}{\tau}\right)H(t)\right]^{1/3}, \quad \omega(t)=\frac{1}{R}\left[\frac{3RW_{\max}}{16g}\left(1+\frac{t}{\tau}\right)H(t)\right]^{2/3}, \tag{6}$$

as well as a pressure profile expressed in terms of time *t* and a radial coordinate *r*:

$$p(r,t)=\frac{4}{\pi R}\int_0^t 2g\exp\left(-\frac{t-\xi}{\tau}\right)\frac{\partial}{\partial\xi}\left(a^2(\xi)-r^2\right)^{1/2}d\xi\,. \tag{7}$$

In the above relations, only the contact radius and the normal approach are obtained in closed-form, whereas the pressure distribution requires numerical treatment. Given these limitations of the existing model, a numerical approach, based on a previous algorithm by the same authors [13], is outlined in the following section, and selected results are used to benchmark the alternate approach.

The derivation of a viscoelastic contact solver is supported by the existence [5] of a numerical model for the contact between bodies of arbitrary profile. The latter model implies discretisation of a limited plane surface around the initial point of contact, resting in the common plane of contact. The algorithm [5] can be applied directly as long as the displacement due to arbitrary pressure distribution can be expressed. The iterative process, mirroring a Conjugate Gradient residual minimisation scheme, gives the contact area as a reunion of discrete elementary cells, and the pressure distribution as a matrix whose elements describe the assumed uniform pressure on each elementary cell.

In the elastic solution, the method of influence coefficients is used to compute, by superposition, the elastic displacement induced in every elementary cell by the pressure elements from all other cells. The viscoelastic case, however, is more complicated because of the time parameter. Based on equation (5) and on the elastic-viscoelastic correspondence principle, a displacement equation is obtained [13], featuring a triple integration:

$$u_3(x_1,x_2,t)=\int_0^t\varphi(t-t')\left[\int_{-\infty}^{\infty}\int_{-\infty}^{\infty}G(x_1-x_1',x_2-x_2')\frac{\partial p(x_1',x_2',t')}{\partial t'}dx_1'dx_2'\right]dt'\,; \tag{8}$$

$$u_3(x_1,x_2,t)=\int_0^t\int_{-\infty}^{\infty}\int_{-\infty}^{\infty}\varphi(t-t')G(x_1-x_1',x_2-x_2')\frac{\partial p(x_1',x_2',t')}{\partial t'}dx_1'dx_2'dt'\,, \tag{9}$$

with x_1 and x_2 rectangular coordinates in the common plane of contact, and *G* the Green's function for the elastic half-space, having the elastic constant $1/(2\mu)$, with μ the shear modulus, removed. The spatial double integration is handled by the discretization applied in the common plane of contact, and the time integration is overcome by finite differences method:

$$\frac{\partial p(x_1',x_2',t')}{\partial t'}dx_1'dx_2'dt'\cong\left(p(x_1',x_2',t'+dt')-p(x_1',x_2',t')\right)dx_1'dx_2'\,. \tag{10}$$

In other words, the loading temporal window is divided into small time segments in which the time dependency is suspended and pressure remains unchanged during the time period. This implies a piecewise constant distribution of pressure over the common plane of contact, and over time as well. With these assumptions, a multi-summation displacement equation is obtained:

$$u_3(i,j,k) = \sum_{n=1}^{N_t} \sum_{\ell=1}^{N_1} \sum_{m=1}^{N_2} \varphi(k-n) G(i-\ell, j-m) \big(p(\ell,m,n) - p(\ell,m,n-1) \big), \quad i = 1 \ldots N_1, j = 1 \ldots N_2, k = 1 \ldots N_t, \tag{11}$$

in which N_1 and N_2 are the numbers of spatial grids and N_t the number of time steps. Relation (11) verifies mathematically the so-called memory effect attributed to viscoelastic materials: viscoelastic displacement attained at a specific time depends on the current pressure distribution, but also on the whole progress of pressure throughout the complete loading window.

Relation (11) allows the estimation of viscoelastic displacement due to arbitrary loading history and, integrated in a contact solver, gives the solution of the viscoelastic contact under both temporal and spatial discretisation. Results obtained with a computer code developed in Matlab, implementing this formulation and used to replicate different contact loading histories, are presented in the following section.

3. RESULTS AND DISCUSSIONS

A rigid ball of radius $R = 0.018$ m is pressed against a viscoelastic half-space described by a Maxwell model with $\tau = 10$ s. Step loading is assumed first, with $W_{max} = 100$ N. The time simulation window is chosen as ratio to the relaxation time. The contact at $t = 0$ is in fact hertzian, and its parameters, $a(0)$, $p_{max}(0)$ and $\omega(0)$ are used as normalizers for their viscoelastic counterparts. In each case, the simulation time is divided into 120 constant steps, and the simulation spatial domain into 256×256 grids. The predictions of the Matlab computer code are depicted using discrete symbols, whereas the data from literature expressions, such as (6) and (7), where available, are displayed with continuous lines. A good match can be seen in figures 1, 2 and 3.

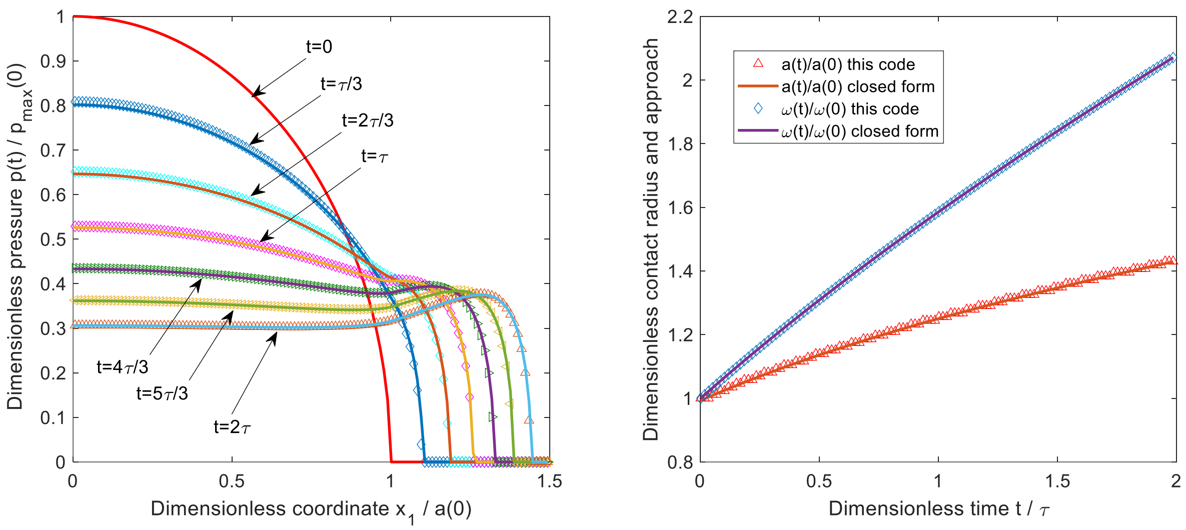

Fig. 1. Contact simulation results in step loading, $t = 2\tau$, and comparison with literature.

A ramped loading is simulated next with the same temporal and spatial discretization. The applied load increases linearly with time, from zero to $W_{max} = 100$ N in a time window of $t = 2\tau$. The contact parameters and the comparison with literature is presented in figure 3.

In the next scenario, the load is ramped down from $W_{max} = 100$ N to zero in a time window of $t = 2\tau$, linearly with time. This case, in which the contact area does not increase monotonically, cannot be treated in the frame of Radok and Lee's framework [1]. Predicted results are plotted in Figure 4, in which the initial contact parameters $a(0)$, $p_{max}(0)$ and $\omega(0)$ are also used as normalizers.

Figure 5 depicts the contact parameters evolution in the case of a sine loading on the first semi-period. Dimensionless loading is defined with respect to load amplitude multiplied by a constant to fit the left y-axis limits, aiming to show the delay between the maximums of load and those of the contact parameters.

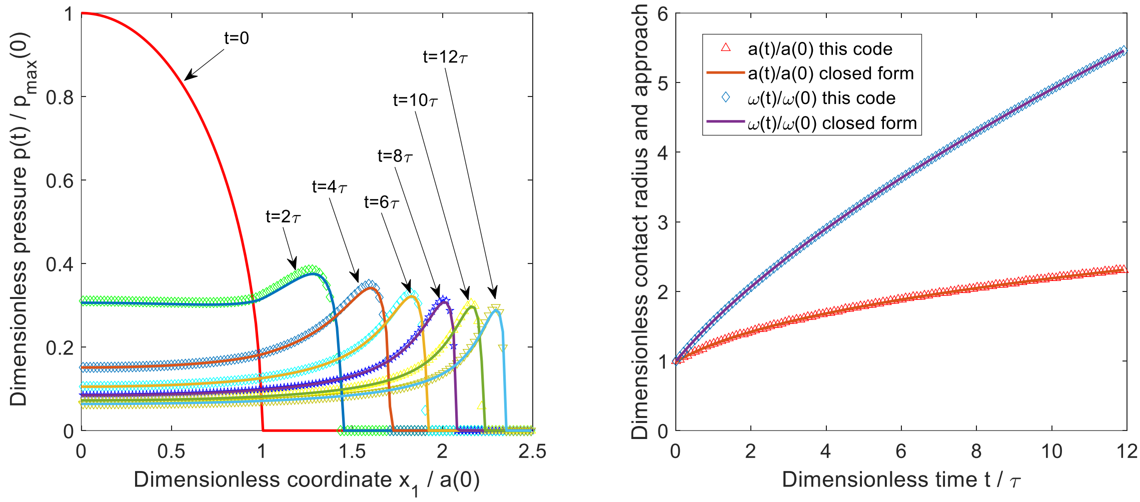

Fig. 2. Contact simulation results in step loading, $t = 12\tau$, and comparison with literature.

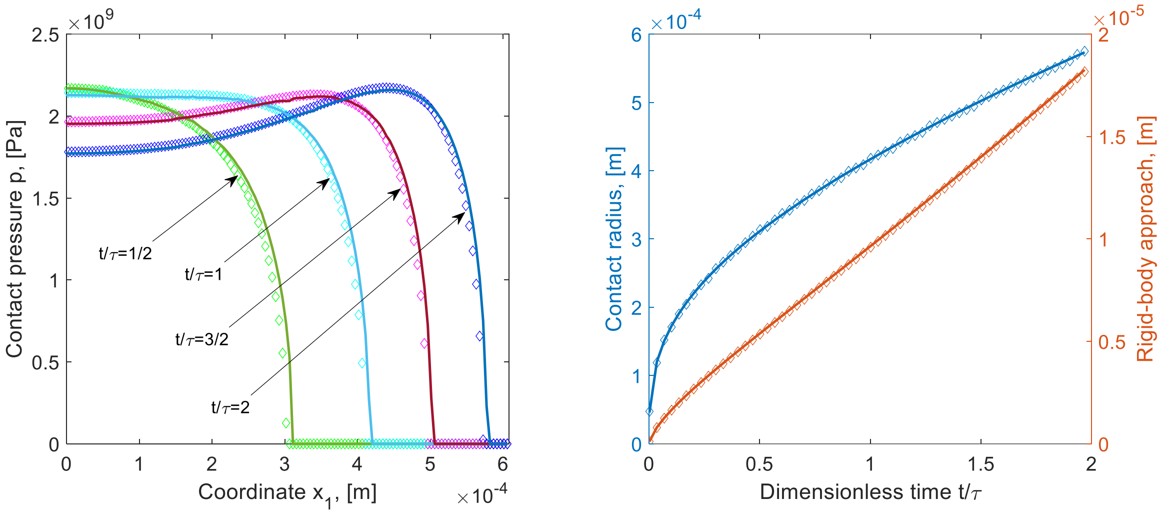

Fig. 3. Contact simulation results in ramped loading, $t = 2\tau$, and comparison with literature.

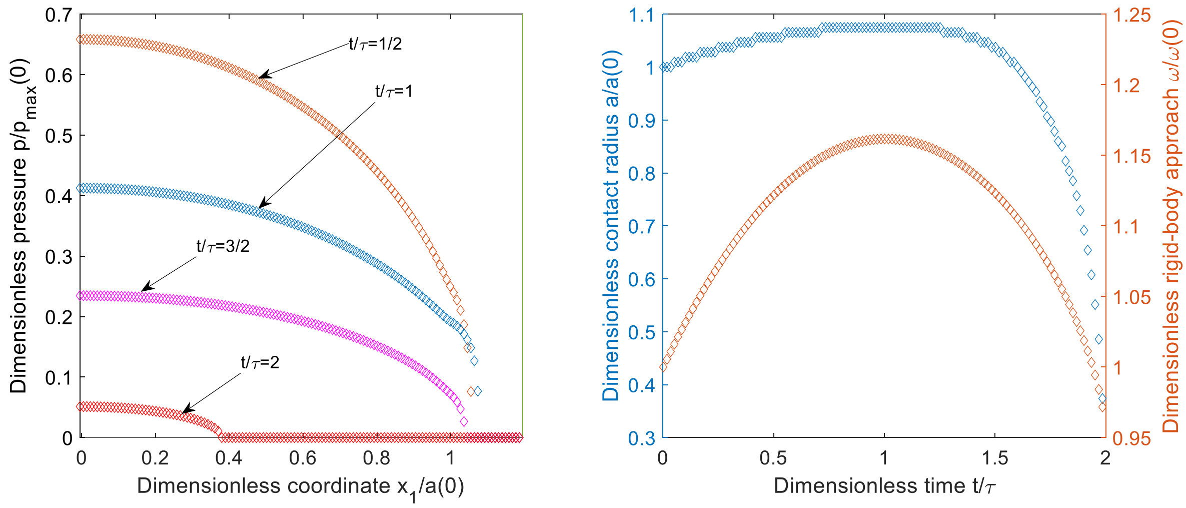

Fig. 4. Contact simulation results in ramped down loading, $t = 2\tau$.

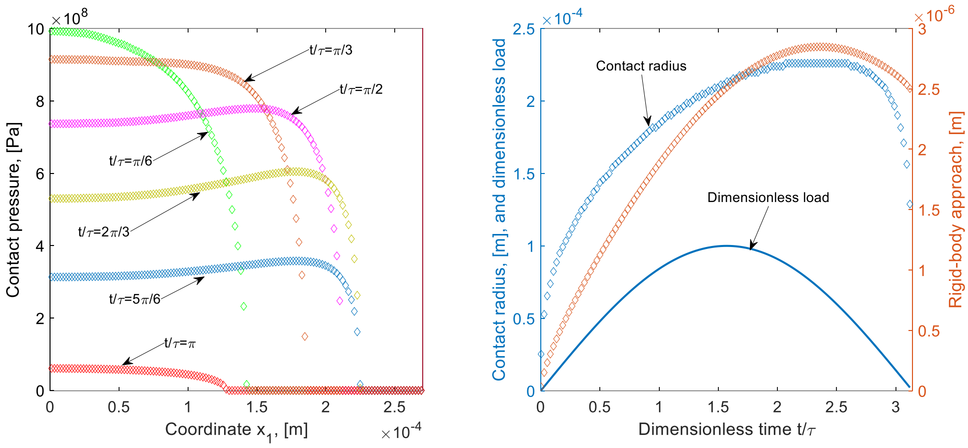

Fig. 5. Contact simulation results in sine loading, $t = \pi\tau$.

A pulsatile loading is then imposed: $W(t) = W_{\max}\left(1-\cos(2\pi\nu t)\right)H(t)$, with $2\pi\nu = 1$ and $\tau = 1$s, and the relation between load frequency, contact area, and rigid-body approach is shown in Figure 6 for the first three load periods. Simulations suggest that, for the considered ratio between the load frequency and the relaxation time of the Maxwell material, a stationary regime is not reached, and, because of out-of-phase response, the contact area and rigid-body approach are expected cu increase with the number of load periods.

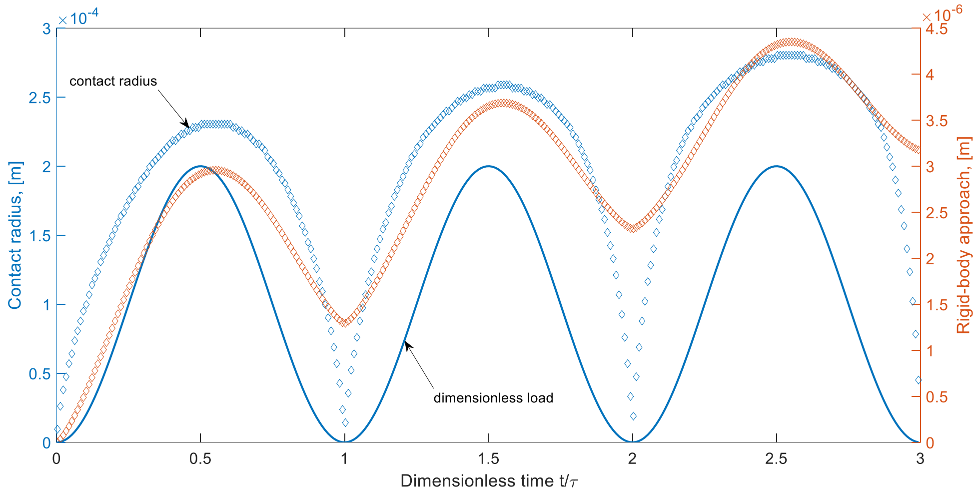

Fig. 5. Contact simulation results in pulsatile loading, $t = 3\tau$.

4. CONCLUSIONS

Maxwell viscoelastic units connected in parallel are essential tools for the modelling of the behaviour of viscoelastic materials. Studying the indentation of a Maxwell viscoelastic half-space is essential to understanding the performance of mechanical contacts involving elastomers or rubber.

Existing models are partially analytical and restricted to monotonically increasing contact areas. Application of semi-analytical methods to the contact of viscoelastic materials yields more general results. A temporal discretization needs to be imposed beside the spatial one to replicate the memory effect of the viscoelastic material. The displacement at any time is calculated as a superposition of effects, involving the current, but also the previous, pressure distribution. Once the pressure-displacement dependence is obtained for arbitrary pressure, an iterative Conjugate Gradient based scheme can provide the contact area and the pressure distribution at any time in the loading window. A computer code is developed to simulate the viscoelastic indentation.

As opposed to elastic materials, viscoelastic results depend on the loading path. Numerous contact simulations are performed, showing the response of the viscoelastic material to various loading histories, including step, ramped, sinusoidal, and pulsatile loads.

Step loading shows initial hertzian behaviour, followed by strong relaxation of central pressure sustained by increasing contact radius. For simulation times exceeding the relaxation time of the Maxwell unit, maximum pressure is moved from the contact axis to the periphery, and central pressure drops to approximately 10% of the initial value. Ramping up the load leads to initial hertzian allure followed by central relaxation of pressure, while the contact radius increases more rapidly than its step loading counterpart. The maximum pressure is also moved from the contact axis to the periphery of the contact area. In both step and ramped up loading, contact area and rigid-body approach increase monotonically with time.

When the load is ramped down, pressure profiles show a Hertzian profile with some perturbations at the periphery. Although the load decreases monotonically, the contact radius and the normal approach are initially increased until the relaxation time is reached, and then decrease to zero. However, at the end of the loading program, i.e. at vanishing load, contact radius and normal approach are not nil, but will further decay with time.

Both sine and pulsatile loads show out-of-phase response between load level, contact radius, and rigid-body approach, proving a hysteretic time exists, which is a source of energy damping in the viscoelastic material. In the case of pulsatile loading, although the load passes through zero and has a continuous slope, a stationary regime is not predicted for the considered ratio between the load frequency and the relaxation time, but it is to be expected for other ratios. A more in-depth study of the indentation load frequency and the energy loss in the viscoelastic contact is left for further studies.

Author contributions: The author confirms the sole responsibility for the conceptualization of the study, methodology, creation of new software used in the paper, validation and visualization of presented results, and manuscript preparation, review, and editing.

Funding source: This paper has received no external funding.

Conflicts of interest: There is no conflict of interest.

5. REFERENCES

1. Lee, E. H., and Radok, J. R. M., (1960). *The Contact Problem for Viscoelastic Bodies*, ASME J. Appl. Mech., 27, 438–444.

2. Hunter, S. C., (1960). *The Hertz Problem for a Rigid Spherical Indenter and a Viscoelastic Half-Space*, J. Mech. Phys. Solids, 8, 219–234.

3. Ting, T. C. T., (1966). *The Contact Stresses Between a Rigid Indenter and a Viscoelastic Half-Space*, ASME J. Appl. Mech., 33, 845–854.

4. Ting, T. C. T., (1968), *Contact Problems in the Linear Theory of Viscoelasticity*, ASME J. Appl. Mech. 35 248–254.

5. Polonsky, I. A., Keer, L. M., (1999). *A Numerical Method for Solving Rough Contact Problems Based on the Multi-Level Multi-Summation and Conjugate Gradient Techniques*, Wear, 231(2), 206-219.

6. Allwood, J. M., (2005). *Survey and Performance Assessment of Solution Methods for Elastic Rough Contact Problems*, ASME J. Tribol., 127(1), 10-23.

7. Jacq, C., Nelias, D., Lormand, G., Girodin, D., (2002). *Development of a Three-Dimensional Semi-Analytical Elastic-Plastic Contact Code*, ASME Journal of Tribology, 124, 653-667.

8. Nélias, D., Antaluca, E., Boucly, V., and Crețu, S., (2007). *A Three-Dimensional Semianalytical Model for Elastic-Plastic Sliding Contacts*, ASME J. Tribol., 129, 761 – 771.

9. Chen, W. W., Wang, Q. J., Huan, Z., Luo, X. (2008). *Semi-Analytical Viscoelastic Contact Modeling of Polymer-Based Materials*, ASME J. Tribol., 133(4), 041404.

10. Vandamme, M., Ulm F.-J., (2005). *Viscoelastic Solutions for Conical Indentation*, International Journal of Solids and Structures, 43(10), 3142-3165.

11. Larsson, P.-L., Carlsson, S.,(1998), *On Microindentation of Viscoelastic Polymers*, Polymer Testing, 17(1), 49-75.

12. Cheng, L. , Xia, X. , Scriven, L.E., Gerberich, W.W., (2005), *Spherical-Tip Indentation of Viscoelastic Material*, Mechanics of Materials, 37(1), 213-226.

13. Spinu, S., and Cerlinca, D., (2017). *Modelling of Rough Contact between Linear Viscoelastic Materials*, Modelling and Simulation in Engineering, 2521903, https://doi.org/10.1155/2017/2521903

14. Ciornei, F. C., (2004). *On the Hertzian Circular Dynamic Contact in the Linear Viscoelastic Domain*, Ph.D. Thesis (in Romanian), University Stefan cel Mare of Suceava, Suceava, Romania.

Received: March 17th, 2025 / Accepted: November 8th, 2025 / Paper available online: December 20th, 2025
© International Journal of Modern Manufacturing Technologies.